Endogenous YAP1 activation drives immediate onset of cervical carcinoma in situ in mice

Nishio, Miki ; To, Yoko ; Maehama, Tomohiko ; Aono, Yukari ; Otani, Junji ; Hikasa, Hiroki ; Kitagawa, Akihiro ; Mimori, Koshi ; Sasaki,…

(Citation)
Cancer Science,111(10):3576-3587

(Issue Date)
2020-10

(Resource Type)
journal article

(Version)
Version of Record

Received: 4 May 2020 | Revised: 15 July 2020 | Accepted: 17 July 2020

DOI: 10.1111/cas.14581

ORIGINAL ARTICLE

Cancer Science WILEY

Endogenous YAP1 activation drives immediate onset of cervical carcinoma in situ in mice

Miki Nishio[1,2] | Yoko To[2,3] | Tomohiko Maehama[1] | Yukari Aono[1] | Junji Otani[1] | Hiroki Hikasa[4] | Akihiro Kitagawa[5] | Koshi Mimori[6] | Takehiko Sasaki[7] | Hiroshi Nishina[8] | Shinya Toyokuni[9] | John P. Lydon[10] | Kazuwa Nakao[11] | Tak Wah Mak[12,13] | Tohru Kiyono[14] | Hidetaka Katabuchi[3] | Hironori Tashiro[15] | Akira Suzuki[1,2]

[1]Division of Molecular and Cellular Biology, Kobe University Graduate School of Medicine, Kobe, Japan

[2]Division of Cancer Genetics, MIB, Kyushu University, Fukuoka, Japan

[3]Department of Obstetrics and Gynecology, Faculty of Life Sciences, Kumamoto University, Kumamoto, Japan

[4]Department of Biochemistry, School of Medicine, University of Occupational and Environmental Health, Kita-kyushu, Japan

[5]Department of Gastroenterological Surgery, Medical School and Graduate School of Frontier Biosciences, Osaka University, Suita, Japan

[6]Department of Surgery, Kyushu University Beppu Hospital, Beppu, Japan

[7]Department of Biochemical Pathophysiology, MRI, Tokyo Medical and Dental University, Tokyo, Japan

[8]Department of Developmental and Regenerative Biology, MRI, Tokyo Medical and Dental University, Tokyo, Japan

[9]Department of Pathology and Biological Responses, Graduate School of Medicine, Nagoya University, Nagoya, Japan

[10]Department of Molecular and Cellular Biology, Baylor College of Medicine, Houston, TX, USA

[11]MIC, Graduate School of Medicine, Kyoto University, Kyoto, Japan

[12]The Princess Margaret Cancer Centre, UHN, Toronto, ON, Canada

[13]Department of Medical Biophysics, Toronto University, Toronto, ON, Canada

[14]Division of Carcinogenesis and Cancer Prevention, National Cancer Center Research Institute, Tokyo, Japan

[15]Department of Women's Health Sciences, Faculty of Life Sciences, Kumamoto University, Kumamoto, Japan

Correspondence
Tomohiko Maehama and Akira Suzuki, Division of Molecular and Cellular Biology, Kobe University Graduate School of Medicine, Kusunoki-cho 7-5-1, Chuo-ku, Kobe, Hyogo 650-0017, Japan.
Emails: tmaehama@med.kobe-u.ac.jp (T.M.); suzuki@med.kobe-u.ac.jp (A.S.)

Hironori Tashiro, Department of Women's Health Sciences, Faculty of Life Sciences, Kumamoto University, Kuhonji 4-24-1, Chuo-ku, Kumamoto 862-0976, Japan.
Email: htashiro@kumamoto-u.ac.jp

Funding information
Japan Agency for Medical Research and Development (Grant/Award Number:

Abstract

Cervical cancer (CC) is usually initiated by infection with high-risk types of human papillomavirus (HPV). The HPV E6 and E7 proteins target p53 and RB, respectively, but other cellular targets likely exist. We generated uterus-specific MOB1A/B double KO (u*Mob1*DKO) mice, which immediately developed cervical squamous cell carcinoma in situ. Mutant cervical epithelial cells showed YAP1-dependent hyperproliferation, altered self-renewal, impaired contact inhibition, and chromosomal instability. p53 activation was increased in u*Mob1*DKO cells, and additional p53 loss in u*Mob1*DKO mice accelerated tumor invasion. In human CC, strong YAP1 activation was observed from the precancerous stage. Human cells overexpressing HPV16 E6/E7 showed inactivation of not only p53 and RB but also PTPN14, boosting YAP1 activation. Estrogen,

Nishio, To and Maehama equally contributed to this study.

"JP20cm0106114"); Cooperative Research Project Program of the MIB, Kyushu University; Japan Society for the Promotion of Science (Grant/Award Number: "17H01400," "26114005," "26640081"); Nanken-Kyoten, Tokyo Medical and Dental University; Kanzawa Medical Research Foundation.

cigarette smoke condensate, and PI3K hyperactivation all increased YAP1 activity in human cervical epithelial cells, and PTPN14 depletion along with PI3K activation or estrogen treatment further enhanced YAP1. Thus, immediate CC onset may initiate when YAP1 activity exceeds an oncogenic threshold, making Hippo-YAP1 signaling a major CC driver.

KEYWORDS

cervical cancer, Hippo-YAP1 pathway, HPV, oncogenic threshold, p53

1 | INTRODUCTION

Cervical cancer (CC) is usually initiated by infection with high-risk types of the human papillomavirus (HPV).[1] Two major histotypes of CC exist: squamous cell carcinomas (SCCs; 80%) and adenocarcinomas (AdCAs; 15-20%).[2] Human cervical SCCs develop from precancerous lesions whose pathology is traditionally graded in three tiers: mild cervical intraepithelial neoplasia (CIN1), CIN2 (moderate) and CIN3 (severe). CIN3 is pathologically very similar to "*carcinoma in situ*" (CIS), leading to the designation CIN3/CIS. CIN2 and CIN3/CIS lesions contain atypical cells with aberrant expression of the HPV oncogenes E6 and E7, often associated with HPV genome integration into the host cell genome.

CC was first combatted through Pap smear screening, followed by HPV vaccination programs that have reduced overall CC incidence.[3] However, CC is still the fourth most common cancer in females, especially in developing countries.[4] Young patients with precancerous lesions usually undergo surgical conization of the cervix to preserve fertility, but then often suffer from adverse reproductive morbidity.[5] Because only 5% of CIN2 and 12%-31% of CIN3/CIS cases progress to invasive CC within 30 years of diagnosis,[6] conization of all precancerous lesions is controversial. A biomarker flagging late-stage lesions would guide physicians considering surgery for young patients. In addition, CC has a poor prognosis in patients with advanced malignancy.[7] However, the generation of biomarkers and new diagnostic/therapeutic strategies is hampered by our lack of understanding of CC's underlying molecular mechanisms.

Within the dividing cells of CIN3/CIS, HPV E6 binds to the cellular ubiquitin ligase E6AP[8] to form a complex targeting p53 for proteasome-mediated degradation, thereby blocking p53-mediated apoptosis.[9] Similarly, HPV E7 binds to retinoblastoma family proteins (RB, p107/RBL1 and p130/RBL2) to promote their degradation,[10,11] abolishing cell cycle control. The inactivation of these two tumor suppressors is crucial for driving CC onset, but because mice lacking RB/p107/p130[12] or p53[13] develop CIS or invasive CC only if exposed to estrogen for 5-6 months, another potent tumorigenic signaling pathway likely contributes to cervical carcinogenesis.

Hippo signaling is activated in response to changes in cell density, external mechanical forces, or rigidity of the extracellular matrix (ECM).[14] The core components of this pathway are mammalian STE20-like protein (MST) kinases, large tumor suppressor homolog (LATS) kinases, and adaptor proteins salvador homolog-1 (SAV1) and mps one binder kinase activator-1 (MOB1).[14] MOB1A/B bind to LATS kinases to strongly increase their activities.[15] The downstream targets of Hippo signaling are the transcriptional cofactors Yes-associated protein-1 (YAP1) and transcriptional coactivator with PDZ-binding motif (TAZ). YAP1 and TAZ bind to proteins in the tight and adherens junctional complexes, including Angiomotin (AMOT),[16] α-Catenin,[17] Protein Tyrosine Phosphatase, Nonreceptor Type 14 (PTPN14),[18] and Scribble.[19] When YAP1/TAZ bind to any of these molecules in a junctional complex, YAP1/TAZ are efficiently phosphorylated by LATS and thereby confined to the cytoplasm, where they are ubiquitinated by E3-ubiquitin ligase $SCF\beta^{TRCP}$ and destroyed by proteasome-mediated degradation.[20] Due to differences in binding partners, the roles of YAP1 and TAZ can differ in some situations.[21,22] In the absence of phosphorylation, however, both YAP1 and TAZ act on TEA domain transcription factors (TEADs) in the nucleus to regulate numerous genes involved in cell growth and differentiation.[23] Thus, in most cell types, YAP1 and TAZ are essentially positive regulators of cell proliferation that are negatively controlled by upstream Hippo core components.

Several lines of evidence suggest YAP1's involvement in CC: (a) location 11q22 in the human *YAP1* locus is amplified in 16% of CCs[24]; (b) mutations of *PIK3CA* (37%), *PTEN* (31%), or *FAT1* (36%),[24-26] which frequently occur in CCs, increase YAP1 activation in other tumor cell types; (c) YAP1 activation is increased in breast cancer cells by estrogen exposure[27] and in human keratinocytes by HPV E6/E7[28]; (d) PAR3, DLG1, SCRIBBLE, MAGI1/3, PTPN14, and p53, all of which are inactivated by HPV E6/E7,[29-31] negatively regulate YAP1 activity in several non-CC tumor cell types[18,19,32,33]; (e) activation of YAP1 or inactivation of LATS1 increases proliferation and invasiveness of CC cell lines[34,35]; (f) LATS1 is downregulated in 45% of CCs[35]; (g) nuclear YAP1 is upregulated in CIN2, CIN3/CIS, and invasive SCC according to some groups[36,37] but not others[38]; (h) transgenic mice with weak activation of an exogenous, constitutively active mutant form of YAP1 [YAP(S127A)] develop invasive CC by age 6-8 months without earlier histological alterations.[37]

To elucidate the role of Hippo signaling in cervical carcinogenesis, we generated and analyzed uterus-specific *Mob1a/1b* null mice.

2 | MATERIALS AND METHODS

The materials and methods listed below are detailed in Document S1, Document S2, and Table S1.

Statistics

Mice

Isolation of TAM-inducible or noninducible primary Mob1 DKO cervical epithelial cells (ipMob1DKO cells)

Immunoblotting

Tissue immunostaining

Clinical samples

BrdU incorporation

TUNEL assay

Cell counts

Colony formation assay

Immunofluorescent visualization of centrosomes and mitotic spindles

Cell size, polyploidy, and aneuploidy

P53 determinations

DNA constructs

Establishment of HCK1T cells with stable protein expression of DNA constructs

MCF10A reporter cell line

siRNA transfections

Effects of estradiol (E2), CSC, and PIK3CA(E545K) on YAP1 activity

Quantitative reverse transcription PCR (qRT-PCR)

Microarray analysis

3 | RESULTS

3.1 | Loss of Mob1a/b triggers early onset of cervical CIS in mice

MOB1 is a core Hippo pathway component and negatively regulates YAP1 activity. To examine the consequences of excessive endogenous YAP1 activity in mouse uterus in vivo, we generated uterus-specific *Mob1a/b* double knockout (DKO) mice. We mated transgenic (Tg) *Progesterone Receptor-Cre Knock-in (PR-Cre)* mice[39] with $Mob1a^{flox/flox}$ and $Mob1b^{-/-}$ mice to generate *PR-Cre*;$Mob1a^{flox/flox}$;$Mob1b^{-/-}$ mice (u*Mob1*DKO mice). Crossing of u*Mob1*DKO mice with *Rosa26-LSL-YFP* reporter mice produced progeny showing YFP positivity in most cervical epithelial cells (CECs) and stromal cells at P7, confirming efficient *Mob1a/1b* deletion (Figure S1A). $Mob1a^{flox/flox}$;$Mob1b^{-/-}$, *PR-Cre*;$Mob1a^{+/+}$;$Mob1b^{+/+}$, and *PR-Cre*;$Mob1a^{flox/flox}$;$Mob1b^{+/+}$ mice were all indistinguishable from wild-type (WT) mice in gross appearance, histology, and survival (Figure S1B), allowing the use of $Mob1a^{flox/flox}$;$Mob1b^{-/-}$ mice as controls in subsequent experiments.

All u*Mob1*DKO mice appeared healthy at birth and most had normal lifespans. However, all u*Mob1*DKO mice developed cervical CIS by P7 (Figure 1A,B). In WT mice, dividing CECs are rare and restricted to the basal epidermis (Figure 1C, upper left, white arrowhead). However, in u*Mob1*DKO mice, CECs showed hyperplasticity and increased division even in nonbasal epidermis (Figure 1A,C, left bottom panel, white arrowheads). Cell polarity was impaired and cell-cell connections were loosened, with some cells detaching by P7 (Figure 1A, red arrowhead). Also by P7, many mutant CECs exhibited abnormally large nuclei and did not resemble typical basal cells (Figure 1C, middle bottom panels, yellow arrowhead). In 3-week-old mutant mice, the cervical epithelial basement membrane had thickened (Figure 1C, right bottom panels, blue arrowheads). By 20 weeks, mutant cervical epithelium showed glandular components in 15% of cases (Figure 1D, upper left). As u*Mob1*DKO mice aged, their CECs rapidly increased in number but did not invade the submucosa until 40 weeks, when the epithelium was convoluted (consistent with CIS). Spontaneous invasive SCCs (Figure 1D, yellow arrowheads) and adenosquamous carcinomas (Figure 1D, lower right) did not develop until 40-60 weeks.

To rule out any effects of uterine stromal cells, and to clarify whether cervical CIS developed if MOB1 was deleted postnatally, we generated mice in which *Mob1a/b* could be inactivated in epithelial cells at any time by tamoxifen (TAM) treatment. We crossed *Keratin14 (K14)-CreERT* Tg mice with $Mob1a^{flox/flox}$;$Mob1b^{-/-}$ mice to produce pe*Mob1*DKO mice (*K14-CreERT*;$Mob1a^{flox/flox}$;$Mob1b^{-/-}$). PCR analysis of control and pe*Mob1*DKO mice confirmed that, by 21 days post-TAM, *Mob1a* was deleted in most *Mob1b*-null CECs (Figure S1C). Like u*Mob1*DKO mice, pe*Mob1*DKO mice developed cervical CIS by day 7 post-TAM (Figure 1E). Because *Mob1a* gene deletion was faintly detectable at day 7 post-TAM (Figure S1C), it seems that CIS appears as soon as this gene is lost in the cervix. All pe*Mob1*DKO mice died at around P28 of malnutrition likely due to dysphasia caused by oral epithelial hyperplasia, precluding further analyses.

The CIS lesions in both u*Mob1*DKO and pe*Mob1*DKO mice affected epithelial cells in both the cervix (including the squamous columnar junction, endocervix, and ectocervix) and vagina but not in the endometrium, despite confirmed MOB1 depletion (Figure 1F, Figure S1A). Thus, upon strong YAP1 activation in cervical squamous cell regions, CIS develops immediately, making dysregulated Hippo-YAP/TAZ signaling a powerful driver of initial CC onset.

3.2 | Tumorigenic anomalies in CECs of uMob1DKO mice

To determine whether MOB1 loss conferred tumorigenicity on CECs, primary *Mob1*DKO CECs were isolated from *Rosa26-CreERT*;$Mob1a^{flox/flox}$;$Mob1b^{-/-}$ mice (*ipMob1*DKO cells). We treated these cells in vitro with (+) or without (–) TAM and examined BrdU incorporation to assess proliferation. Compared with control *ipMob1*DKO–TAM cells, *ipMob1*DKO+TAM cells showed increased BrdU uptake (Figure 2A). TUNEL-positive

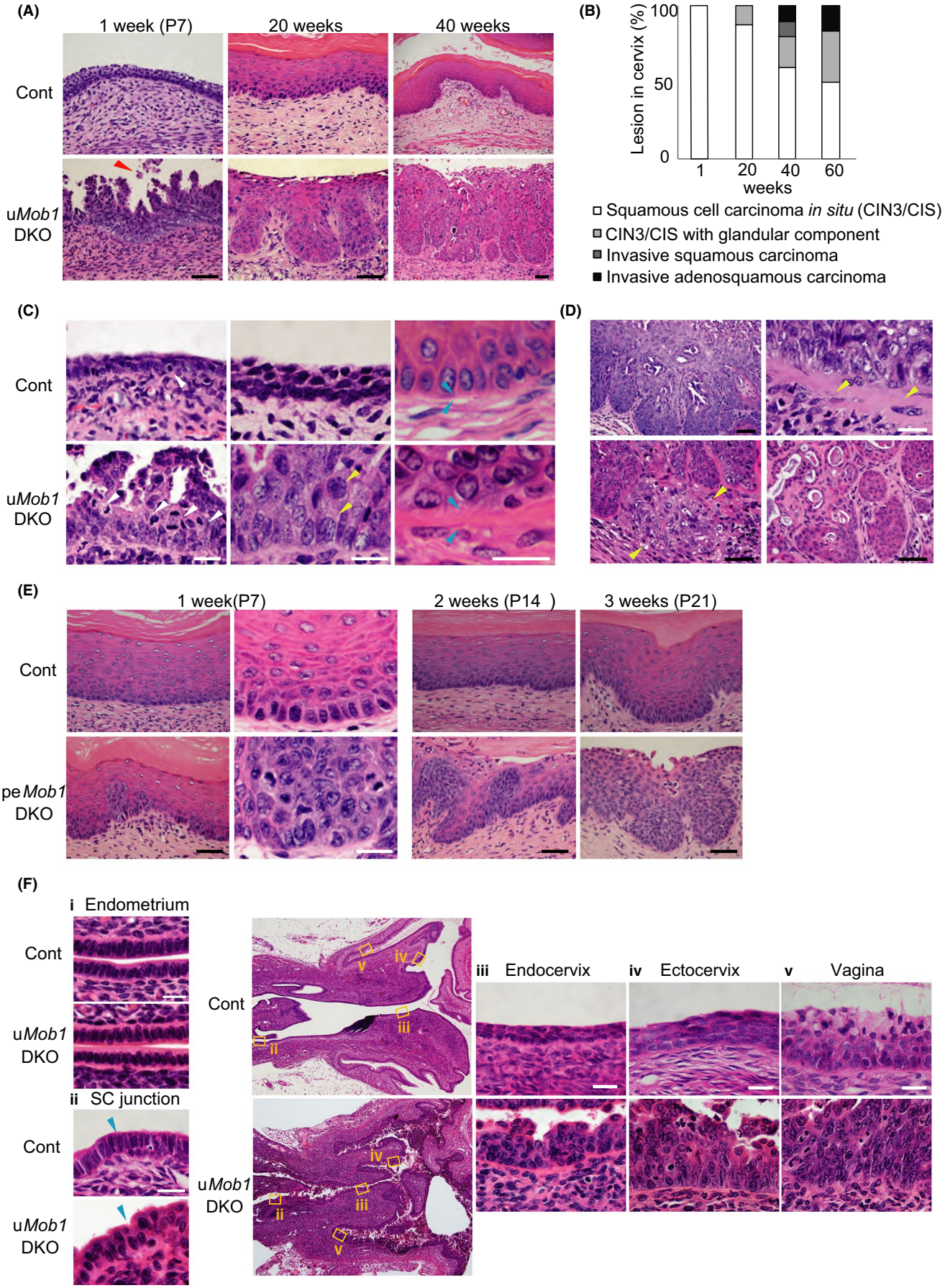
(A)
1 week (P7)
20 weeks
40 weeks
Cont
uMob1 DKO
(B)
Lesion in cervix (%)
100
50
0
1
20
40
60
weeks
Squamous cell carcinoma in situ (CIN3/CIS)
CIN3/CIS with glandular component
Invasive squamous carcinoma
Invasive adenosquamous carcinoma
(C)
Cont
uMob1 DKO
(D)
(E)
1 week(P7)
2 weeks (P14)
3 weeks (P21)
Cont
peMob1 DKO
(F)
i Endometrium
Cont
uMob1 DKO
ii SC junction
Cont
uMob1 DKO
iii Endocervix
iv Ectocervix
v Vagina

FIGURE 1 Histological analyses of cervical epithelial sections from control and Mob1a/b-deficient mice. A, Representative H&E-stained cervical tissues from control (*Mob1a*$^{flox/flox}$;*Mob1b*$^{-/-}$) and u*Mob1*DKO mice (n = 20 mice/group/timepoint) sacrificed at the indicated weeks after birth. Actively growing papillary carcinoma in situ (CIS) was observed in all u*Mob1*DKO mice at P7. Red arrowhead, detaching cells. For all panels, white scale bars, 20 μm; black scale bars, 50 μm. B, Percentages of the u*Mob1*DKO mice in (A) showing the indicated grades of cervical tumors at the indicated weeks after birth. C, High magnification images of cervical sections from u*Mob1*DKO mice. Increased cell division at P7 (white arrowheads), enlarged nuclei at P14 (yellow arrowhead), and thickened basement membrane at 10 wk (blue arrowheads) are shown. D, Left top: Representative cervical CIS with a rete ridge-like glandular component in a 20-week-old u*Mob1*DKO mouse. Right top: Cancer cells invading the basement membrane at 40 wk (yellow arrowheads). Left bottom: Cancer cells under submucosal tissue at 40 wk (yellow arrowheads). Right bottom: Invasive SCC with glandular component (adenosquamous carcinoma) at 55 wk. E, Representative H&E-stained cervical tissues from control (*Mob1a*$^{flox/flox}$;*Mob1b*$^{-/-}$) and pe*Mob1*DKO mice sacrificed at the indicated weeks after birth (n = 10 mice/group/timepoint). F, Representative H&E-stained sections of the indicated tissues (i-iv) from control (*Mob1a*$^{flox/flox}$;*Mob1b*$^{-/-}$) and u*Mob1*DKO mice at P21

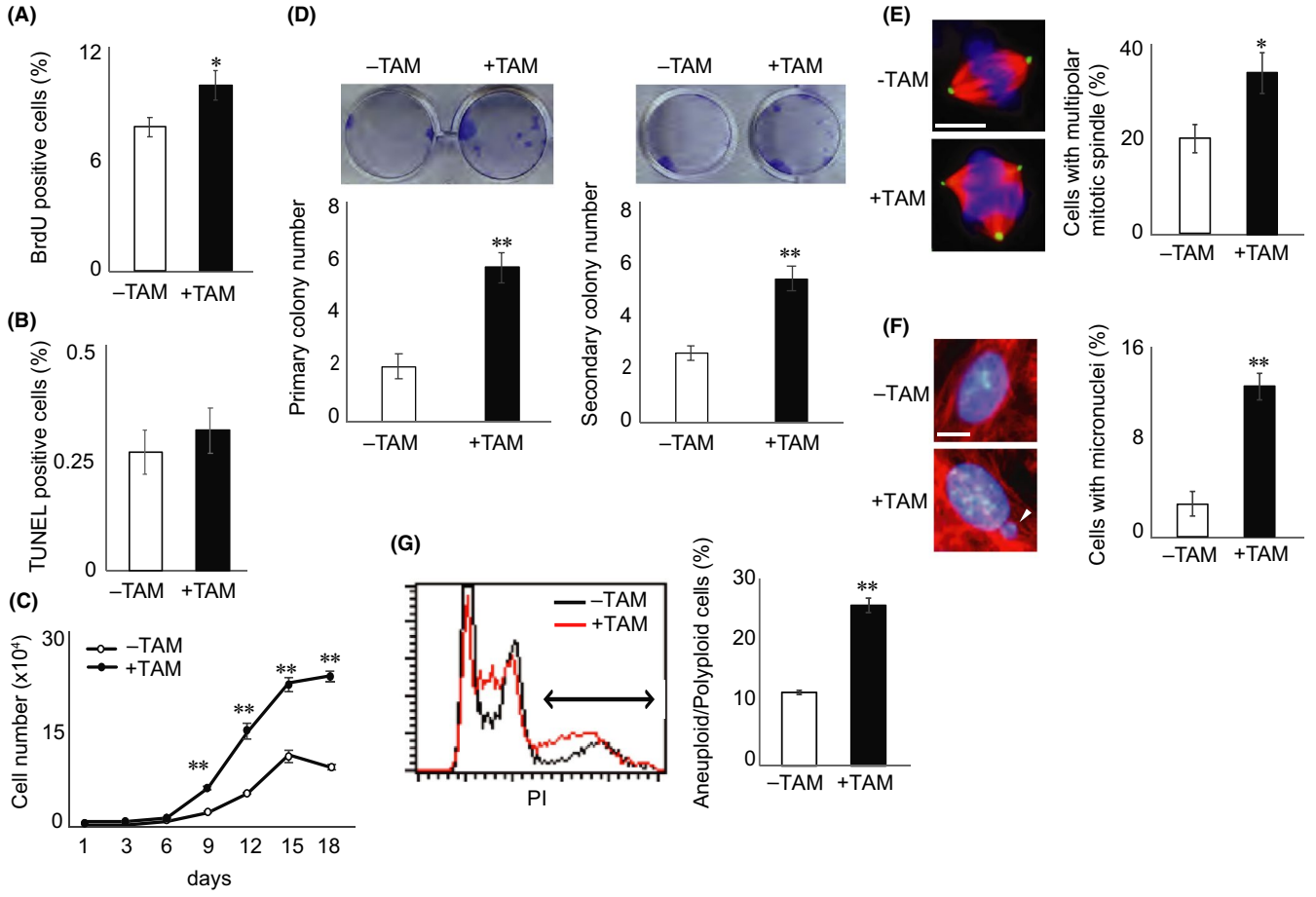

FIGURE 2 Tumorigenic properties of MOB1-deficient cervical epithelial cells (CECs). A, Quantitation of percentages of BrdU^{+} cells in cultures of *ipMob1*DKO cells that were cultured with (*Mob1*DKO) or without (control) tamoxifen (TAM). For all panels, data are the mean ± SEM (n = 3). B, Quantitation of TUNEL^{+} cells in *ipMob1*DKO cultures grown with/without TAM. C, Total cell numbers of *ipMob1*DKO cells grown with/without TAM for the indicated days. D, Colony formation by *ipMob1*DKO cells cultured with/without TAM. Primary (left) and secondary (right) colonies were stained and counted. E, Left: Immunostaining to detect γ-tubulin (green) and α-tubulin (red) in *ipMob1*DKO cells grown with/without TAM. DAPI (blue), chromosomes. Scale bar, 5 μm. Right: Quantitation of multipolar cells. F, Left: DAPI staining revealing increased micronuclei (arrowhead) in *ipMob1*DKO cells grown with TAM. Scale bar, 5 μm. Right: Quantitation of cells harboring micronuclei. G, Left: Flow cytometric analysis to detect cell ploidy in PI-stained spontaneously immortalized *ipMob1*DKO cells grown with/without TAM. Right: Quantitation of aneuploid plus polyploid cells

cells indicating spontaneous apoptosis were barely detectable regardless of TAM (Figure 2B). Cell-plating studies demonstrated that the saturation density of *ipMob1*DKO+TAM cells was also increased (Figure 2C). Because FACS analysis revealed no cell size difference between *ipMob1*DKO−TAM and *ipMob1*DKO+TAM cells (Figure S1D), the heightened saturation density of the MOB1-depleted culture suggested impaired cell-cell contact inhibition.

To determine whether MOB1 inactivation affected the self-renewal of cervical epithelial stem cells, we quantified the ability of

*ipMob1*DKO cells to form primary colonies in culture. MOB1 depletion induced a 2.5-fold increase in colony-forming efficiency (Figure 2D, left panel). When these MOB1-deficient primary colonies were replated, a 2.2-fold increase in secondary colony-forming efficiency was observed (Figure 2D, right panel).

We next analyzed chromosomal instability associated with MOB1 deficiency. Immunofluorescent analysis revealed a higher percentage of *ipMob1*DKO+TAM cells with multipolar spindles, indicating defective chromosomal segregation (Figure 2E). Cells harboring micronuclei (cytoplasmic chromosomal fragments generated by aberrant mitosis) were also increased in *ipMob1*DKO+TAM cultures (Figure 2F). FACS analysis of spontaneously immortalized *ipMob1*DKO+TAM cells revealed increased aneuploid and/or polyploid (>4N) cells (Figure 2G). Thus, MOB1 inactivation enhances hyperproliferation, impairs cell-cell contact inhibition, increases self-renewal, and promotes chromosomal instability, likely accounting for the early cancers in u*Mob1*DKO mice.

3.3 | Enhanced YAP1/TAZ activation in MOB1-deficient cervical epithelial cells

As expected, *ipMob1*DKO+TAM cells at maximum saturation density showed reduced total LATS1, decreased YAP1 (Ser127) phosphorylation, and increased total YAP1 and total TAZ proteins (Figure 3A), with no differences in phospho-MST1 or total MST1. Immunostaining of P7 u*Mob1*DKO cervical tissues showed increased staining intensity in the nucleus and cytoplasm of mutant YAP1^{+} cells (Figure 3B). CECs with elevated nuclear YAP were mainly located in the basal layer in control mice but in the basal and suprabasal layers in u*Mob1*DKO mice.

To investigate YAP1/TAZ's role in the phenotypes of MOB1-deficient CECs, we used *K14-CreERT* Tg mice to generate triple KO mutants either lacking YAP1 plus MOB1 [*K14-CreERT*;*Mob1a*$^{flox/flox}$;*Mob1b*$^{-/-}$;*Yap1*$^{flox/flox}$; designated pe*Mob1Yap1*TKO] or lacking TAZ plus MOB1 [*K14-CreERT*;*Mob1a*$^{flox/flox}$;*Mob1b*$^{-/-}$;*Taz*$^{flox/flox}$;

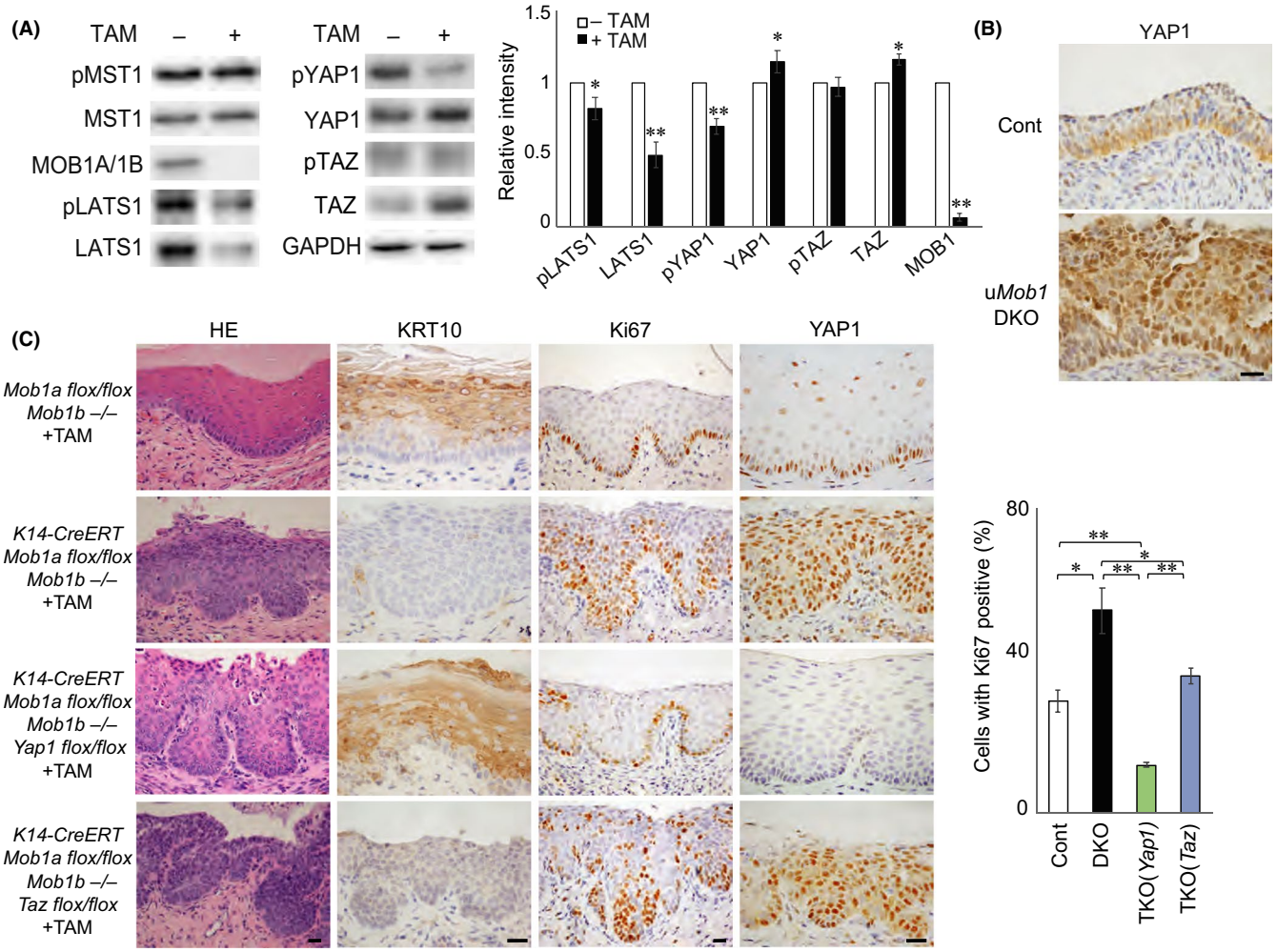

FIGURE 3 Mps one binder kinase activator-1 (MOB1)-mediated regulation of Yes-associated protein-1 (YAP1) controls cervical epithelial cell (CEC) homeostasis. A, Left: Immunoblot to detect the indicated Hippo pathway proteins in *ipMob1*DKO cells cultured with/without tamoxifen (TAM). GAPDH, loading control. Right: Quantitation of relative staining intensities of proteins in the left panel. B, Representative immunostaining to detect YAP1 protein in control and u*Mob1*DKO cervical epithelium at P7 (n = 3). Scale bar, 20 μm. C, Left: Representative immunostaining to detect Keratin-10 (KRT10), Ki67 and YAP1 in cervical epithelium of mice of the indicated genotypes at 4 wk after TAM treatment for 5 d. Scale bars, 20 μm. Right: Quantitation of percentage of Ki67^{+} cells in the sections in the left panel

designated pe*Mob1Taz*TKO]. Indeed, MOB1-deficient CECs were largely rescued by additional YAP1 deficiency and partially rescued by TAZ deficiency (Figure 3C), indicating that phenotypes associated with MOB1 deficiency depend more strongly on YAP1 than TAZ.

3.4 | MOB1-deficient cervical CIS cells show p53 activation that inhibits cancer progression

The postmitotic antiproliferative effects associated with aneuploidy are partly due to p53 induction and activation of the DNA damage response (DDR).[40] Cervical CIS cells from P21 u*Mob1*DKO mice showed heightened γH2AX and p53 activation (Figure 4A,B), indicating that the increased p53 in mutant tissues may be caused by DDR. MOB1-deficient cells with large nuclei, abnormal centrosome number, or micronuclei also showed increased p53 (Figure 4C). Thus, DDR induced by chromosomal instability triggers p53 induction in *Mob1*DKO cervical CIS cells.

To examine this finding in vivo, we generated MOB1-deficient mice that were also either heterozygous (*Tp53* Het/*Mob1*DKO) or homozygous (*Tp53* Homo/*Mob1*DKO) for mutant p53. By age 15 weeks, 30% of *Tp53* Het/*Mob1*DKO mice and 65% of *Tp53* Homo/*Mob1*DKO mice had developed invasive cervical SCCs (Figure 4D). These malignancies were never observed in either 15-week-old u*Mob1*DKO mice expressing WT p53 or *Tp53* Homo/*Mob1*WT mice. Thus, MOB1-deficient cervical CIS cells may stay in the CIS stage for long periods partly due to the increased p53 induced by the DDR triggered by chromosomal instability.

3.5 | YAP1 activation in human cervical lesions

We next determined YAP1 immunostaining intensity in normal human cervical epithelial tissues as well as in samples from patients with CIN1, CIN2, or CIN3/CIS (Figure 5, upper panel). Significant YAP1 activation (greater than score 2; see Figure 5, right panel) occurred in 75% of CIN1 samples and in 100% of CIN2 and CIN3/CIS samples. The mean YAP1

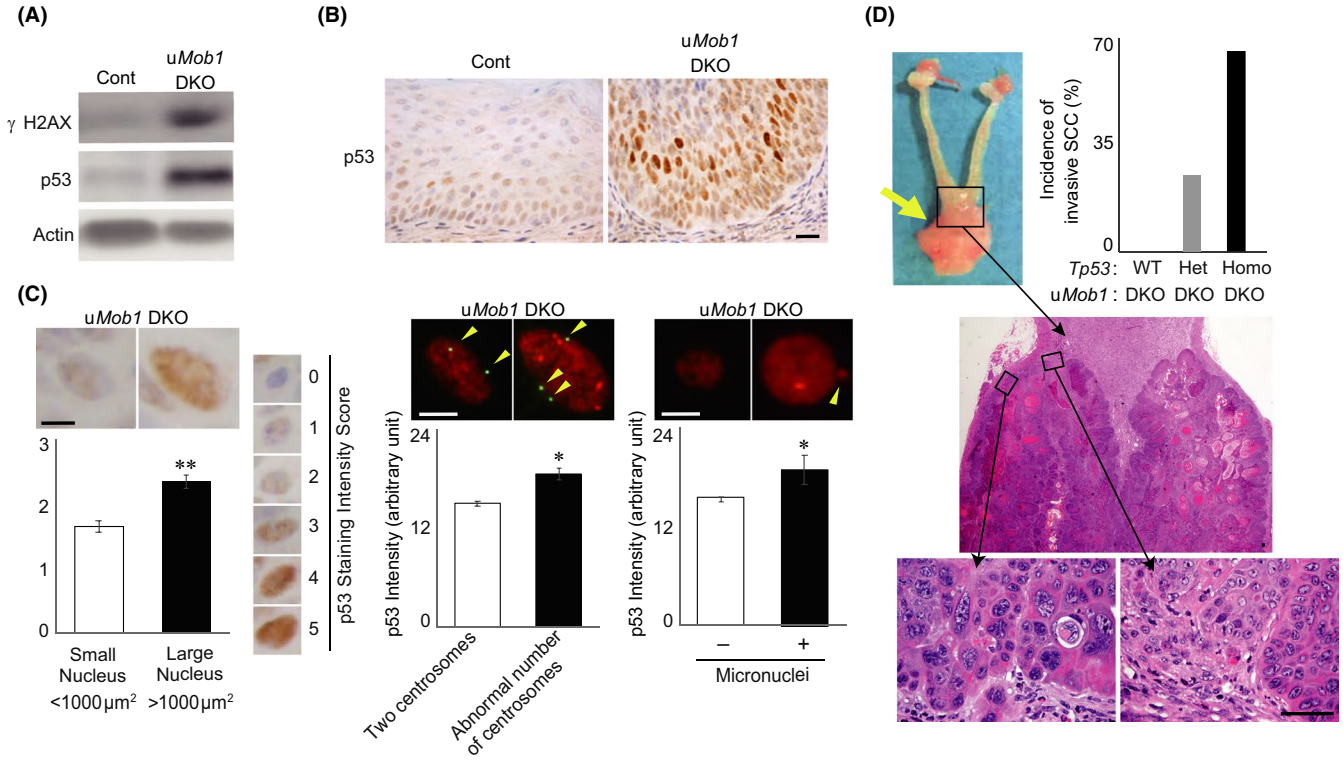

FIGURE 4 MOB1-deficient cervical carcinoma in situ (CIS) cells show inhibited progression due to increased p53. A, Immunoblot to detect γH2AX and p53 in (cervical epithelial cells) CECs from 3-week-old control and u*Mob1*DKO mice (n = 3). Actin, loading control. B, Representative immunostaining to detect p53 in cervical epithelium of control and u*Mob1*DKO mice at P49 (n = 3). Scale bar, 20 μm. C, Left top: Representative immunostaining to detect p53 in u*Mob1*DKO CECs (counterstain: hematoxylin). For all panels: scale bars, 5 μm. Left bottom: Quantitation of p53 staining intensity (see indicated chart) correlated with nuclear size. Middle top: Staining to detect p53 (red) and γ-tubulin (green) in u*Mob1*DKO CECs with 1, 2, or multiple centrosomes (arrowheads). Middle bottom: Quantitation of p53 staining intensity in u*Mob1*DKO CECs with the indicated number of centrosomes. Right top: Staining to detect p53 (red) in u*Mob1*DKO CECs with/without micronuclei (arrowhead). Right bottom: Quantitation of p53 staining intensity in u*Mob1*DKO CECs with/without micronuclei. D, Top left: Representative macroscopic view of invasive cervical cancer (CC) (arrow) in a 15-week-old *Tp53* Homo/*Mob1*DKO mouse. Middle: Low magnification image of the CC in the top left panel. Bottom: High magnification images of H&E-stained sections of (left) enlarged nuclei and (right) cancer cell invasion in boxed areas of the middle panel. Scale bars, 20 μm. Top right: Quantitation of percentages of mice with the indicated genotypes (n = 10/group) showing cervical squamous cell carcinoma (SCC) by 15 wk of age

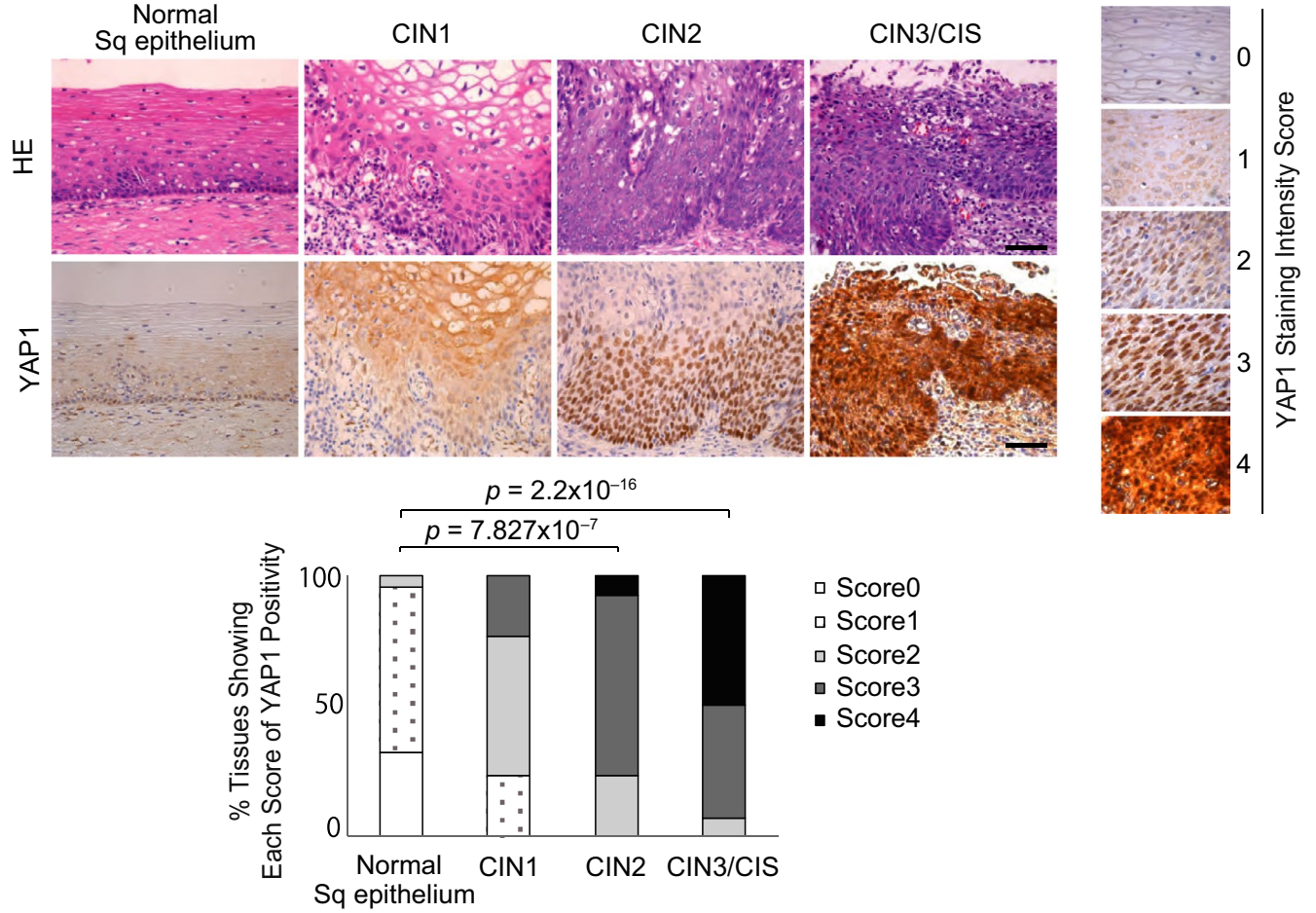

FIGURE 5 Activation of Yes-associated protein-1 (YAP1) in human cervical lesions. Top left: Representative H&E-stained sections of normal human cervical squamous (Sq) epithelium and human CIN1, CIN2 and CIN3/CIS. Middle left: YAP1 immunostaining of the sections in the top panels. Scale bars, 50 μm. Right: YAP1 activity scoring panel. For the tissue samples in the middle panel, YAP1 scores were as follows: nontumorous tissue = 0, CIN1 = 1, CIN2 = 3, and CIN3/CIS = 4. Bottom left: Quantitation of percentages of the indicated sample types showing the indicated YAP1 activity scores. *P* values, Chi-square test. CIN, cervical intraepithelial neoplasia; CIS, carcinoma in situ

staining intensity score was significantly higher in CIN2 and CIN3/CIS samples than in normal samples, and only 3% of normal samples showed detectable YAP1 activation (Figure 5, lower panels). Thus, significant YAP1 activation begins in human CC starting at the precancerous, moderately dysplastic stage (CIN2).

3.6 | HPV E6/E7, PTPN14 degradation, E2, CSC, and PI3K activate YAP1 and contribute to the onset of human CCs

Inactivation of MAGI1/3, PAR3, DLG1, SCRIB, p53, or PTPN14 by HPV E6 or E7 increases YAP activity.[18,19,29-33] We separately transfected siRNAs directed against these HPV targets into our previously established MCF10A reporter cells designed to reflect YAP1/TAZ transcriptional activity in vitro.[41] Suppression of *PTPN14* mRNA boosted YAP1 reporter activity much more than did knockdown of other E6/E7 target genes (Figure 6A, Figure S2A-H). *PTPN14* siRNA also induced significant accumulation of YAP1 protein in immortalized human CECs (HCK1T cells)[42] (Figure 6B).

CC-related carcinogens such as estrogen (E2) and cigarette smoke condensate (CSC) increase intracellular YAP1 protein in noncervical cells.[27,43] We found that these agents also activate YAP1 in human CECs (Figure 6C, left panel). HCK1T cells expressing Dox-inducible forms of either HPV E6/E7 or the constitutively active PIK3CA(E545K) mutation, which is observed from the CIN3 stage,[25,27] showed enhanced YAP1 activation (Figure 6C), confirming a previous report.[44] In addition, we found that PTPN14 suppression plus either PIK3CA(E545K) expression or estrogen treatment additively increased YAP1 target gene expression (Figure 6D).

HPV16 E6/E7 inactivate PTPN14, p53, and RB1 in human epithelial cells and CC cell lines.[9-11,31] Accordingly, HCK1T cells expressing Dox-inducible E6/E7 (HCK1TiE6E7 cells) showed decreased PTPN14, p53, and RB1 proteins but increased YAP1 protein (Figure 6E). Thus, it is mainly HPV's targeting of PTPN14 that boosts YAP1 activation and enhances cellular proliferation. Indeed, E6/E7 overexpression in HCK1T cells greatly increased their proliferation in vitro in a manner largely prevented by treatment of these cells with *YAP1* siRNA (but not *TAZ* siRNA) (Figure 6F). *YAP1* siRNA plus

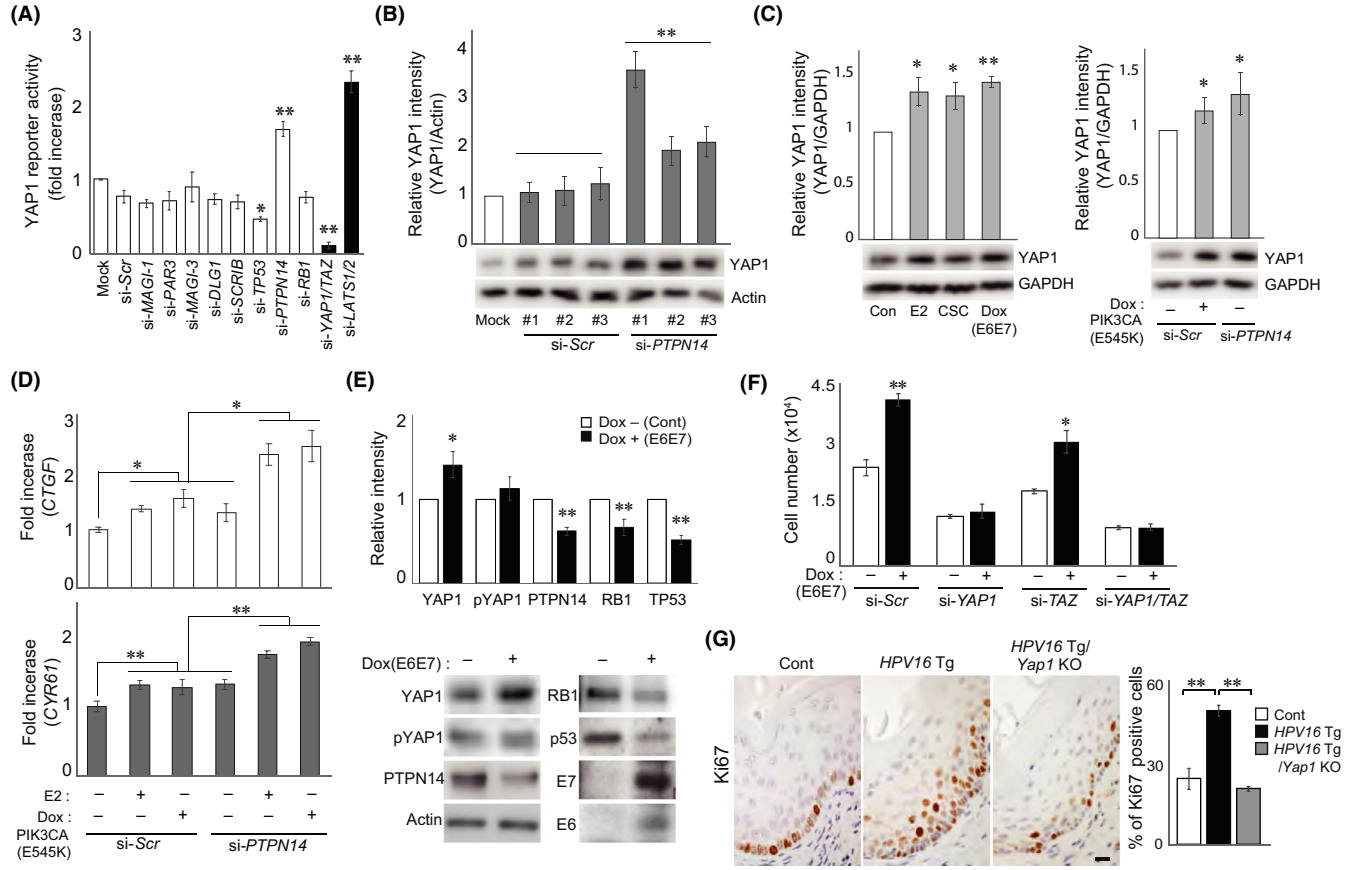

FIGURE 6 Contributions of the human papillomavirus (HPV) E6/E7, PTPN14 degradation, E2, cigarette smoke condensate (CSC), and PI3K to Yes-associated protein-1 (YAP1) activation during the onset of human cervical cancers. A, Quantitation of relative YAP1 activity in MCF10A reporter cells transfected separately for 2 d with the indicated siRNAs. B, Quantitation of immunoblot to detect YAP1 in HCK1T cells treated for 2 d with control siRNA (si-Scr) or siRNA targeting *PTPN14* (si-*PTPN14*). C, Quantitation of immunoblots to detect YAP1 in (left) HCK1T-iE6E7 cells cultured for 24 h with estradiol (E2, 1μM), CSC (10 μg/mL), or Dox (1 μg/mL, to induce E6/E7 expression), and in (right) HCK1T-PIK3CA(E545K) cells cultured for 12 h with/without Dox [to induce PIK3CA(E545K) expression]. si-*Scr*#1 or si-*PTPN14*#1 treatment was performed 24 h before Dox application. D, Quantitation of expression of the YAP1 target genes *CTGF* and *CYR61* in HCK1T-PIK3CA(E545K) cells that were cultured for 12 h with estradiol (E2, 1 μM) or Dox (1 μg/mL). siRNA treatment was performed 12 h before Dox application. E, Quantitation of immunoblot to detect YAP1 activation as well as inactivation of the E6/E7 target proteins PTPN14, RB1, and p53 in HCK1T-iE6E7 cells that were cultured with (black) or without (white) Dox for 3 d to induce E6E7 expression. F, Total cell numbers in cultures of HCK1T cells that were: transfected with vector expressing Dox-inducible HPV E6/E7; precultured with (black) or without (white) Dox for 3 d; and replated (1×10^4/well) in 48-well plates, with (black) or without (white) Dox plus the indicated siRNAs for 4 d. G, Left: Representative Ki67 staining of cervical epithelium from control, *HPV16*Tg and *HPV16Tg/Yap1*KO mice at 8 wk after tamoxifen (TAM) administration. Scale bar, 20 μm. Right: Quantitation of percentage of Ki67$^+$ cells in the sections in the left panels

TAZ siRNA completely rescued these cells. Lastly, in cervical tissues of Tg mice expressing HPV16 under the control of the K14 promoter (*HPV16* Tg mice),[45] the percentage of Ki67$^+$ proliferating CECs was increased (Figure 6G). This in vivo effect was abolished in cervical tissues of *HPV16* Tg *Yap1* KO mice (Figure 6G).

YAP1-induced failure of innate immune responses and Type 1 IFN production reportedly explains the initiation and progression of CCs.[37] However, our RT-PCR (Figure S3A) and IHC (Figure S3B) analyses of CECs from 3-week-old u*MOB1*DKO mice revealed no deficits in innate immunity or IFN production. mRNA levels of Mx1, a downstream target of IFN, were not significantly different from controls, and levels of Isg15, another downstream target of IFN, were actually increased. YAP1 activation in these mutant CECs was confirmed by the increased expression of the known YAP1 target genes *Ctgf* and *Cyr61*. Thus, CIS onset in u*MOB1*DKO mice is indifferent to failure of innate immunity but absolutely requires YAP1 activation.

Collectively, our data suggest that HPV E6/E7 may promote human CEC proliferation mainly by inducing PTPN14 degradation, which ultimately results in YAP1 activation. YAP1 activation is accelerated by estrogen, CSC, or mutant PIK3CA, leading to CC onset. Moreover, the inhibition of p53 by HPV E6 may facilitate CC development into invasive SCC.

4 | DISCUSSION

Surprisingly, endogenous YAP1 activation due to MOB1A/B deficiency induces immediate onset of murine cervical CIS comparable

to human CIN3/CIS. HPV16 E6/E7, estrogen, CSC, and mutant PIK3CA all induce YAP1 activation in CECs (Figure 6C,D), suggesting that the Hippo-YAP1 pathway is the master signaling mechanism driving CC carcinogenesis (Figure S4). Indeed, human CIN2 cells expressing integrated E6/E7 genes showed significant YAP1 activation, with human CIN3/CIS cells displaying even stronger YAP1 activation (Figure 5). YAP1 activation is thus an important driver of HPV-induced CIS formation, and invasive CC may arise upon sustained YAP1 activation and/or other molecular alterations such as loss of p53 or RB.

DNA alterations other than HPV E6/E7 integration are rarely found in human CIN3 cells. PIK3CA is the only mutated gene ever detected in human CIN3 lesions, in just 5.4% of cases.[25] Interestingly, DNA mutations of Hippo signaling components are relatively rare in human malignancies[46] despite the frequent presence of high YAP1 protein levels. These observations imply that YAP1 expression may be epigenetically altered during tumorigenesis, perhaps explaining why the importance of Hippo-YAP1 signaling in CC onset was hidden for so long.

Our results have shed much-needed new light on mechanisms involved in CIS formation.

(1) *HPV E6/E7*: Among E6/E7 target genes, PTPN14 had by far the strongest effect on YAP1 activation (Figure 6A). Although PTPN14 inhibition had been previously shown to activate YAP1 in noncervical cell types, our work is the first to demonstrate that PTPN14 is elevated in CECs (Figure 6B). Thus, an E6/E7-PTPN14-YAP1 axis appears crucial for the onset of human cervical CIN3/CIS. Because Tg mice expressing E6/E7 alone do not develop CIS,[47] the integration of multiple HPV genomes, stronger transcription of HPV E6/E7, and/or greater YAP1 activation due to additional exposure to carcinogens or PIK3CA activation may be needed to exceed the YAP1 oncogenic threshold for CIS formation (Figure S4).

(2) *Estrogen*: While it was known that estrogen activates YAP1 in breast cancer cells,[27] we have now demonstrated that the same is true in estrogen-treated CECs. Our data provide a basis for the positive correlation of a large number of full-term pregnancies, or a long duration of oral contraceptive use, with elevated CIN3/CIS or CC risk in humans.[48] Conversely, CIN3/CIS regression is frequently observed postpartum, when estrogen levels drop.[49] In HPV Tg mouse models, estrogen promotes cervical carcinogenesis.[50] Thus, in addition to E6/E7, estrogen appears to be a significant contributor to the YAP1 activation critical for cervical CIN3/CIS onset and progression.

(3) *CSC*: Epidemiological studies have established that tobacco smoke facilitates HPV-mediated CC initiation and progression.[51] Acute CSC exposure triggers phosphorylation and activation of EGFR, which promotes PI3K/AKT/c-JUN-induced E6/E7 transcription.[52] In addition, nicotine reportedly activates YAP1 in esophageal SCC.[43] We have clarified that CSC activates YAP1 in CECs (Figure 6C), implying that smoking may exacerbate CIN3/CIS onset.

(4) *Mutated PIK3CA*: In noncervical epithelial cells, activation of YAP1 by PI3K is controversial.[44,53] We have confirmed that constitutive activation of PIK3CA definitely activates YAP1 in CECs (Figure 6C,D). Even without PIK3CA mutation, the PI3K pathway can be activated in CECs by various growth factors, estrogen, or CSC,[44] setting the stage for CIS onset and CC development.

Our u*Mob1*DKO mice immediately developed cervical papillary CIS that did not pass through the CIN1 and CIN2 stages typical of human cervical lesions. These murine papillary CIS either grew into the cervical lumen (outside) or formed a nest in the cervical stroma (inside), similar to the glandular involvement seen in human CIN3/CIS. However, these malignant cells in u*Mob1*DKO mice did not invade the submucosa until age 40 weeks (Figure 1A,B). The evolution of CIN3/CIS into invasive SCC likely involves the accumulation of epigenetic and genetic changes in oncogenes and tumor suppressor genes. One reason for the delayed appearance of invasive SCC in u*Mob1*DKO mice may be the elevated activated p53 in the mutant cells. Because they were often aneuploid, MOB1-deficient CECs exhibited focal γH2AX and p53 activation that inhibited cell proliferation and the development of advanced cancer. However, HPV targets not only YAP1/TAZ but also p53 for degradation.[9] Thus, HPV may turn a cervical CIN3/CIS into an invasive carcinoma faster than does altered Hippo signaling. Indeed, our *Tp53* Homo/*Mob1*DKO mice showed earlier onset of invasive tumors than did u*Mob1*DKO mice (Figure 4D).

A second reason for the slow development of SCC in u*Mob1*DKO mice may be the increased production of ECM elements, especially fibronectin, by mutant CECs (Figure S5). This reinforced barrier, along with the increased thickness of the cervical epithelial basal membrane (Figure 1C), could help to protect submucosal tissues from tumor cell invasion in our mutant mice. Note, however, that the cervical epithelial basal membrane is not obviously thicker in human CIS samples.

A recent report by He et al[37] described Tg mice whose keratinocytes weakly expressed a constitutively active form of YAP1 [YAP(S127A)] in TAM-inducible fashion. These mutants developed invasive cervical SCC by 6-8 months after YAP activation. However, there was no mention at all about the development of CIS in these mice. In contrast, our mice exhibited strongly activated endogenous YAP in PR- or K14-expressing CECs and developed cervical CIS immediately after YAP activation. Thus, we have shown that sustained YAP can drive CIS in the absence of any other molecular alteration. On the other hand, both He et al and we observed a lag of several months in SCC development after YAP activation, implying that other genetic or epigenetic alterations are required for the onset of invasive SCC.

Another difference between our study and that of He et al concerns the involvement of innate immunity in CC onset. He et al showed that the innate immune response was decreased in 10-month-old YAP Tg mice bearing advanced SCCs. In contrast, our qPCR and IHC analyses of 3-week-old WT control, MOB1B-deficient, and MOB1A/B DKO mice showed no decreases in expression of innate immune response genes (Figure S3). Thus, a failure in innate immunity does not contribute to CIS onset in u*Mob1*DKO mice, whereas endogenous YAP1 hyperactivation is essential.

Our study can lay claim to the following novel findings:

1. Mob1 depletion leading to endogenous YAP hyperactivation in mouse uterus induces the immediate onset of cervical CIS. This phenotype was prevented by depletion of YAP1 (but not TAZ), pinpointing YAP as the key molecule driving CIS with no need for any other gene alteration. We therefore propose a new concept positing that human cervical CIN3/CIS simply initiates when sustained YAP1 activity exceeds a particular oncogenic threshold.
2. We also demonstrated that YAP activation is associated with chromosomal instability that upregulates p53, and that if this YAP activation occurs when p53 is inactivated, advanced cancers can develop.
3. Many CC risk factors reportedly increase YAP activity, but we are the first to directly compare these risk factors using YAP reporter cells. We found that PTPN14-activated downstream of E6/E7 was the strongest YAP activator, and that various combinations of these risk factors cause additive accumulation of activated YAP.

Our work has produced mice that can serve as a suitable model for further study of the mechanisms underlying CC onset and progression. We also recently generated mice lacking MOB1 specifically in the tongue (t*Mob1*DKO mice). Like CC onset in u*Mob1*DKO mice, tongue cancer onset in t*Mob1*DKO mutants is observed within 1 week of gene ablation.[54] We therefore propose that Hippo-YAP1 signaling may be a master pathway that universally drives CIS formation in squamous cells. Our mutant animals may provide useful platforms for the exploration of new drugs designed to combat cancers mediated by altered Hippo signaling, including CC. Our data also imply that measuring YAP1 and p53 activity in human CIN2 or CIN3/CIS may be of diagnostic value. p53 expression is lower in human CIN3 cases than in CIN2 patients and higher in CIN3/CIS cases that regress than in those that persist.[55,56] Thus, assessment of YAP and p53 in CIN2 or CIN3/CIS cells may assist physicians in selecting those high-risk patients who will actually benefit from conization, sparing others from surgical overtreatment.

ACKNOWLEDGMENTS

We thank J. Wrana (Lunenfeld-Tanenbaum Research Institute) for Tazflox/flox mice. We are grateful for the funding provided by the Japanese Society for the Promotion of Science (JSPS; grants 17H01400, 26114005, 26640081); the Cooperative Research Project Program of the MIB, Kyushu University; Nanken-Kyoten, Tokyo Medical and Dental University (TMDU); the Japanese Agency for Medical Research and Development [P-CREATE(AMED) grant; JP20cm0106114]; and the Kanzawa Medical Research Foundation.

DISCLOSURE

The authors have no conflicts of interest to declare.

ETHICAL APPROVAL

Animal experiments were approved by the Kobe University and Kyushu University Animal Experiment Committees, and the care of the animals was in accordance with institutional guidelines. All clinical samples were approved for analysis by the Ethics Committee at the Kumamoto University and Kyushu University.

ORCID

Koshi Mimori https://orcid.org/0000-0003-3897-9974
Shinya Toyokuni https://orcid.org/0000-0002-5757-1109
Tohru Kiyono https://orcid.org/0000-0003-1769-403X
Hironori Tashiro https://orcid.org/0000-0001-6236-2849
Akira Suzuki https://orcid.org/0000-0002-5950-8808

REFERENCES

1. Munoz N, Bosch FX, de Sanjose S, et al. Epidemiologic classification of human papillomavirus types associated with cervical cancer. *N Engl J Med*. 2003;348:518-527.
2. Silverberg SG, Ioffe OB. Pathology of cervical cancer. *Cancer J*. 2003;9:335-347.
3. Luostarinen T, Apter D, Dillner J, et al. Vaccination protects against invasive HPV-associated cancers. *Int J Cancer*. 2018;142:2186-2187.
4. Bray F, Ferlay J, Soerjomataram I, Siegel RL, Torre LA, Jemal A. Global cancer statistics 2018: GLOBOCAN estimates of incidence and mortality worldwide for 36 cancers in 185 countries. *CA Cancer J Clin*. 2018;68:394-424.
5. Bevis KS, Biggio JR. Cervical conization and the risk of preterm delivery. *Am J Obstet Gynecol*. 2011;205:19-27.
6. McCredie MR, Sharples KJ, Paul C, et al. Natural history of cervical neoplasia and risk of invasive cancer in women with cervical intraepithelial neoplasia 3: a retrospective cohort study. *Lancet Oncol*. 2008;9:425-434.
7. Cohen PA, Jhingran A, Oaknin A, Denny L. Cervical cancer. *Lancet*. 2019;393:169-182.
8. Origoni M, Cristoforoni P, Carminati G, et al. E6/E7 mRNA testing for human papilloma virus-induced high-grade cervical intraepithelial disease (CIN2/CIN3): a promising perspective. *Ecancermedicalscience*. 2015;9:533.
9. Crook T, Tidy JA, Vousden KH. Degradation of p53 can be targeted by HPV E6 sequences distinct from those required for p53 binding and trans-activation. *Cell*. 1991;67:547-556.
10. Dyson N, Howley PM, Munger K, Harlow E. The human papilloma virus-16 E7 oncoprotein is able to bind to the retinoblastoma gene product. *Science*. 1989;243:934-937.
11. Boyer SN, Wazer DE, Band V. E7 protein of human papilloma virus-16 induces degradation of retinoblastoma protein through the ubiquitin-proteasome pathway. *Cancer Res*. 1996;56:4620-4624.
12. Shin MK, Sage J, Lambert PF. Inactivating all three rb family pocket proteins is insufficient to initiate cervical cancer. *Cancer Res*. 2012;72:5418-5427.
13. Shai A, Pitot HC, Lambert PF. p53 Loss synergizes with estrogen and papillomaviral oncogenes to induce cervical and breast cancers. *Cancer Res*. 2008;68:2622-2631.
14. Nakatani K, Maehama T, Nishio M, et al. Targeting the Hippo signalling pathway for cancer treatment. *J Biochem*. 2017;161:237-244.
15. Moreno CS, Lane WS, Pallas DC. A mammalian homolog of yeast MOB1 is both a member and a putative substrate of striatin family-protein phosphatase 2A complexes. *J Biol Chem*. 2001;276:24253-24260.
16. Chan SW, Lim CJ, Chong YF, Pobbati AV, Huang C, Hong W. Hippo pathway-independent restriction of TAZ and YAP by angiomotin. *J Biol Chem*. 2011;286:7018-7026.
17. Schlegelmilch K, Mohseni M, Kirak O, et al. Yap1 acts downstream of alpha-catenin to control epidermal proliferation. *Cell*. 2011;144:782-795.

18. Wang W, Huang J, Wang X, et al. PTPN14 is required for the density-dependent control of YAP1. *Genes Dev*. 2012;26:1959-1971.
19. Mohseni M, Sun J, Lau A, et al. A genetic screen identifies an LKB1-MARK signalling axis controlling the Hippo-YAP pathway. *Nat Cell Biol*. 2014;16:108-117.
20. Zhao B, Li L, Tumaneng K, Wang CY, Guan KL. A coordinated phosphorylation by Lats and CK1 regulates YAP stability through SCF(beta-TRCP). *Genes Dev*. 2010;24:72-85.
21. Plouffe SW, Lin KC, Moore JL 3rd, et al. The Hippo pathway effector proteins YAP and TAZ have both distinct and overlapping functions in the cell. *J Biol Chem*. 2018;293:11230-11240.
22. Callus BA, Finch-Edmondson ML, Fletcher S, Wilton SD. YAPping about and not forgetting TAZ. *FEBS Lett*. 2019;593:253-276.
23. Zhao B, Ye X, Yu J, et al. TEAD mediates YAP-dependent gene induction and growth control. *Genes Dev*. 2008;22:1962-1971.
24. Cancer Genome Atlas Research Network, Albert Einstein College of Medicine, Analytical Biological Services, et al. Integrated genomic and molecular characterization of cervical cancer. *Nature*. 2017;543:378-384.
25. Verlaat W, Snijders PJ, van Moorsel MI, et al. Somatic mutation in PIK3CA is a late event in cervical carcinogenesis. *J Pathol Clin Res*. 2015;1:207-211.
26. Martin D, Degese MS, Vitale-Cross L, et al. Assembly and activation of the Hippo signalome by FAT1 tumor suppressor. *Nat Commun*. 2018;9:2372.
27. Zhou X, Wang S, Wang Z, et al. Estrogen regulates Hippo signaling via GPER in breast cancer. *J Clin Invest*. 2015;125:2123-2135.
28. Webb Strickland S, Brimer N, Lyons C, Vande Pol SB. Human Papillomavirus E6 interaction with cellular PDZ domain proteins modulates YAP nuclear localization. *Virology*. 2018;516:127-138.
29. Ganti K, Broniarczyk J, Manoubi W, et al. The human papillomavirus E6 PDZ binding motif: from life cycle to malignancy. *Viruses*. 2015;7:3530-3551.
30. Takizawa S, Nagasaka K, Nakagawa S, et al. Human scribble, a novel tumor suppressor identified as a target of high-risk HPV E6 for ubiquitin-mediated degradation, interacts with adenomatous polyposis coli. *Genes Cells*. 2006;11:453-464.
31. White EA, Munger K, Howley PM. High-risk human papillomavirus E7 proteins target PTPN14 for degradation. *MBio*. 2016;7:e01530-16.
32. Mello SS, Valente LJ, Raj N, et al. A p53 super-tumor suppressor reveals a tumor suppressive p53-Ptpn14-Yap axis in pancreatic cancer. *Cancer Cell*. 2017;32(4):460-473.e6.
33. Zhang P, Wang S, Wang S, et al. Dual function of partitioning-defective 3 in the regulation of YAP phosphorylation and activation. *Cell Discov*. 2016;2:16021.
34. Lorenzetto E, Brenca M, Boeri M, et al. YAP1 acts as oncogenic target of 11q22 amplification in multiple cancer subtypes. *Oncotarget*. 2014;5:2608-2621.
35. Deng J, Zhang W, Liu S, An H, Tan L, Ma L. LATS1 suppresses proliferation and invasion of cervical cancer. *Mol Med Rep*. 2017;15:1654-1660.
36. Xiao H, Wu L, Zheng H, et al. Expression of Yes-associated protein in cervical squamous epithelium lesions. *Int J Gynecol Cancer*. 2014;24:1575-1582.
37. He C, Lv X, Huang C, et al. A human papillomavirus-independent cervical cancer animal model reveals unconventional mechanisms of cervical carcinogenesis. *Cell Rep*. 2019;26(10):2636-2650.e5.
38. Liu T, Liu Y, Gao H, Meng F, Yang S, Lou G. Clinical significance of yes-associated protein overexpression in cervical carcinoma: the differential effects based on histotypes. *Int J Gynecol Cancer*. 2013;23:735-742.
39. Soyal SM, Mukherjee A, Lee KY, et al. Cre-mediated recombination in cell lineages that express the progesterone receptor. *Genesis*. 2005;41:58-66.
40. Ohashi A, Ohori M, Iwai K, et al. Aneuploidy generates proteotoxic stress and DNA damage concurrently with p53-mediated post-mitotic apoptosis in SAC-impaired cells. *Nat Commun*. 2015;6:7668.
41. Nishio M, Sugimachi K, Goto H, et al. Dysregulated YAP1/TAZ and TGF-beta signaling mediate hepatocarcinogenesis in Mob1a/1b-deficient mice. *Proc Natl Acad Sci USA*. 2016;113:E71-E80.
42. Yugawa T, Handa K, Narisawa-Saito M, Ohno S, Fujita M, Kiyono T. Regulation of Notch1 gene expression by p53 in epithelial cells. *Mol Cell Biol*. 2007;27:3732-3742.
43. Zhao Y, Zhou W, Xue L, Zhang W, Zhan Q. Nicotine activates YAP1 through nAChRs mediated signaling in esophageal squamous cell cancer (ESCC). *PLoS One*. 2014;9:e90836.
44. Fan R, Kim NG, Gumbiner BM. Regulation of Hippo pathway by mitogenic growth factors via phosphoinositide 3-kinase and phosphoinositide-dependent kinase-1. *Proc Natl Acad Sci USA*. 2013;110:2569-2574.
45. Arbeit JM, Munger K, Howley PM, Hanahan D. Progressive squamous epithelial neoplasia in K14-human papillomavirus type 16 transgenic mice. *J Virol*. 1994;68:4358-4368.
46. Harvey KF, Zhang X, Thomas DM. The Hippo pathway and human cancer. *Nat Rev Cancer*. 2013;13:246-257.
47. Park JS, Rhyu JW, Kim CJ, et al. Neoplastic change of squamo-columnar junction in uterine cervix and vaginal epithelium by exogenous estrogen in hpv-18 URR E6/E7 transgenic mice. *Gynecol Oncol*. 2003;89:360-368.
48. Roura E, Travier N, Waterboer T, et al. The influence of hormonal factors on the risk of developing cervical cancer and pre-cancer: results from the EPIC cohort. *PLoS One*. 2016;11:e0147029.
49. Schuster S, Joura E, Kohlberger P. Natural history of squamous intraepithelial lesions in pregnancy and mode of delivery. *Anticancer Res*. 2018;38:2439-2442.
50. Chung SH, Franceschi S, Lambert PF. Estrogen and ERalpha: culprits in cervical cancer? *Trends Endocrinol Metab*. 2010;21:504-511.
51. Fonseca-Moutinho JA. Smoking and cervical cancer. *ISRN Obstet Gynecol*. 2011;2011:847684.
52. Munoz JP, Carrillo-Beltran D, Aedo-Aguilera V, et al. Tobacco exposure enhances human papillomavirus 16 oncogene expression via EGFR/PI3K/Akt/c-Jun signaling pathway in cervical cancer cells. *Front Microbiol*. 2018;9:3022.
53. Basu S, Totty NF, Irwin MS, Sudol M, Downward J. Akt phosphorylates the Yes-associated protein, YAP, to induce interaction with 14-3-3 and attenuation of p73-mediated apoptosis. *Mol Cell*. 2003;11:11-23.
54. Omori H, Nishio M, Masuda M, et al. YAP1 is a potent driver of the onset and progression of oral squamous cell carcinoma. *Sci Adv*. 2020;6:eaay3324.
55. Baak JP, Kruse AJ, Robboy SJ, Janssen EA, van Diermen B, Skaland I. Dynamic behavioural interpretation of cervical intraepithelial neoplasia with molecular biomarkers. *J Clin Pathol*. 2006;59:1017-1028.
56. Ghosh D, Roy AK, Murmu N, Mandal S, Roy A. Risk categorization with different grades of cervical pre-neoplastic lesions - high risk HPV associations and expression of p53 and RARbeta. *Asian Pac J Cancer Prev*. 2019;20:549-555.

SUPPORTING INFORMATION

Additional supporting information may be found online in the Supporting Information section.

How to cite this article: Nishio M, To Y, Maehama T, et al. Endogenous YAP1 activation drives immediate onset of cervical carcinoma in situ in mice. *Cancer Sci*. 2020;111:3576–3587. https://doi.org/10.1111/cas.14581